AN EARTHQUAKE SOURCE SENSITIVITY ANALYSIS FOR TSUNAMI PROPAGATION IN THE EASTERN MEDITERRANEAN

BY ÖCAL NECMIOĞLU AND NURCAN M. ÖZEL

ABSTRACT. Accurate earthquake source parameters are essential input to tsunami hazard assessment and mitigation, including early warning systems. It is difficult to make accurate assumptions of earthquake source parameters where the tectonic setting is complex. To develop a better understanding of the relationship between tsunami impact and earthquake source, it is necessary to investigate variations in all parameters controlling the tsunami. This study investigates the sensitivity of earthquake source parameters in tsunami generation and propagation, with special focus on the Eastern Mediterranean. Our analysis shows that, given the difficulty in accurately determining all focal mechanism parameters, tsunami hazard studies should look at a range of parameters, taking into consideration the maximum generated tsunami. If this broad study scope is not possible due to computational limitations, at least sensitivity studies, such as presented here, should be conducted, and parameters should be selected that would lead to maximum tsunami generation. An option would be to consider only strike and rake variations in the scenario databases as the key criteria in determining the worst-case scenario for a given forecast point.

INTRODUCTION

Information on tsunamigenic sources in the Eastern Mediterranean is of crucial importance, especially considering the relatively short distances between earthquake sources and tsunami arrivals in this region. To overcome the difficulties caused by fast tsunami arrival times, Boğaziçi University's Kandilli Observatory and Earthquake Research Institute (KOERI) is initiating an extensive modeling study with the aim of producing a tsunami hazard map for the Eastern Mediterranean, Aegean, and Black Seas. The goal of this initiative is not only to review existing tsunami zones and re-evaluate existing studies but also to concentrate on regions where such hazard assessments have not previously been made. Each tsunami source region will be modeled using a deterministic approach, and a tsunami hazard map for the Eastern Mediterranean, Aegean, and Black Seas will be created (Ozel et al., 2011). The study presented here is a preliminary step toward creation of such a tsunami hazard map.

UNCERTAINTIES IN EARTHQUAKE SOURCE PARAMETERS

Different physical processes control tsunami generation, propagation, and interaction with the coast. Accurate earthquake source parameters are essential input to tsunami hazard assessment and mitigation, including early warning systems. These parameters are very important to consider, especially in the absence of high-resolution coastal bathymetric data. Here, we study the degrees of uncertainty in the earthquake source parameters in terms of their effects on tsunami generation and propagation. Fault orientation is characterized by its strike (Φ; the azimuth of the fault's projection onto the surface measured from the north), dip (δ; angle between Earth's surface and the fault plane), and rake (λ; the direction of the slip vector measured in the fault plane) at its hypocenter defined by latitude, longitude, and depth. In addition to the length (L), width (W), and slip (u) of the faults, the source parameters are especially important in determining the actual seafloor displacement that results from fault movement in Earth's crust. In real life, and for each new earthquake source, many, if not all, such parameters are expected to vary (Okal and Synolakis, 2004).

The T (minimum compressive stress), P (maximum compressive stress), and B (intermediate stress or null) axes of earthquake moment tensors are often used to evaluate regional stress directions and other tectonic parameters, but up to 15° uncertainty should be expected (Frohlich and Davis, 1999). Satake (1985) studied the effects of station distribution and focal mechanism on moment tensor inversion by means of numerical experiment. In his study, far-field displacements of P waves and Rayleigh waves computed from fault models were inverted to the moment tensor after the error corresponding to the observation error was added to the displacement; experiments were conducted for both ideal and actual station coverage distributions. Results showed that for the actual station distribution, the root-mean-square (rms) errors vary significantly with the location and event mechanism for the actual station distribution. Thus, these experiments indicate that station coverage seriously affects moment tensor inversion, and hence special care should be taken in interpreting these routinely determined results. This is still a live issue in seismology, especially considering that a uniform global station distribution has not yet been achieved.

In an attempt to characterize uncertainties in earthquake focal mechanism parameters, Hellfrich (1997) looked at differences between the parameters derived by different organizations for the same earthquake. He based the uncertainties on the expected mechanism correlation coefficient for different earthquake depths or sizes, and found that small, shallow earthquake focal mechanisms are less likely to correlate well than deep, large ones. In fact, when we look at the focal mechanisms provided by different catalogs for our study area (Figure 1), we observe a certain degree of mismatch between the data sets. In Figure 1, moment tensor catalogs are presented according to the fault type classification of Zoback (1992), given in Table 1. While the maps displayed here do not provide the one-to-one earthquake comparison suggested by Hellfrich (1997), it is clear that the interpretation of the fault mechanism based on different moment tensor catalogs may lead to different conclusions.

The initial tsunami wave carries the most valuable information about its source, especially regarding bathymetry, which affects the initial wave's shape and velocity (Yolsal and Taymaz, 2010). Okal (1988) explained that earthquake source depth plays only a minor role in tsunami generation, showing that tsunami wave amplitude is reduced by a factor of two when focal depth ranges from 20 km to 100 km. The effects of earthquake location in the far and near fields have also been studied (Okal, 1988; Gica et al., 2007; Okal and Synolakis, 2008) as one of the commonly accepted crucial earthquake parameters determining the characteristics of final tsunami waves arriving at the coasts (Yolsal and Taymaz, 2010). Abe and Okada (1995) indicated the importance of fault area size on tsunami spectra in numerical simulations. They suggested that increasing the fault length contributes to a large predominant period, while also increasing the fault width accelerates sharpness of the spectral peak. However, other studies conducted by Titov et al. (1999) and Okal and Synolakis (2008) implied that tsunami waves exhibit minor sensitivity to the dimensions of the rupture plane in the far field. Several numerical experiments conducted by Titov et al. (1999) studied the influence of small variations in dip and rake angles on tsunami waves. They indicated that lowering the dip angle from 20° to 10° led to a 30% decrease in the amplitudes of leading tsunami waves, whereas

Öcal Necmioğlu (ocal.necmioglu@boun.edu.tr) is PhD Candidate, Kandilli Observatory and Earthquake Research Institute, Boğaziçi University, Istanbul, Turkey. **Nurcan M. Özel** is Professor and Head, Department of Geophysics, Boğaziçi University, Istanbul, Turkey.
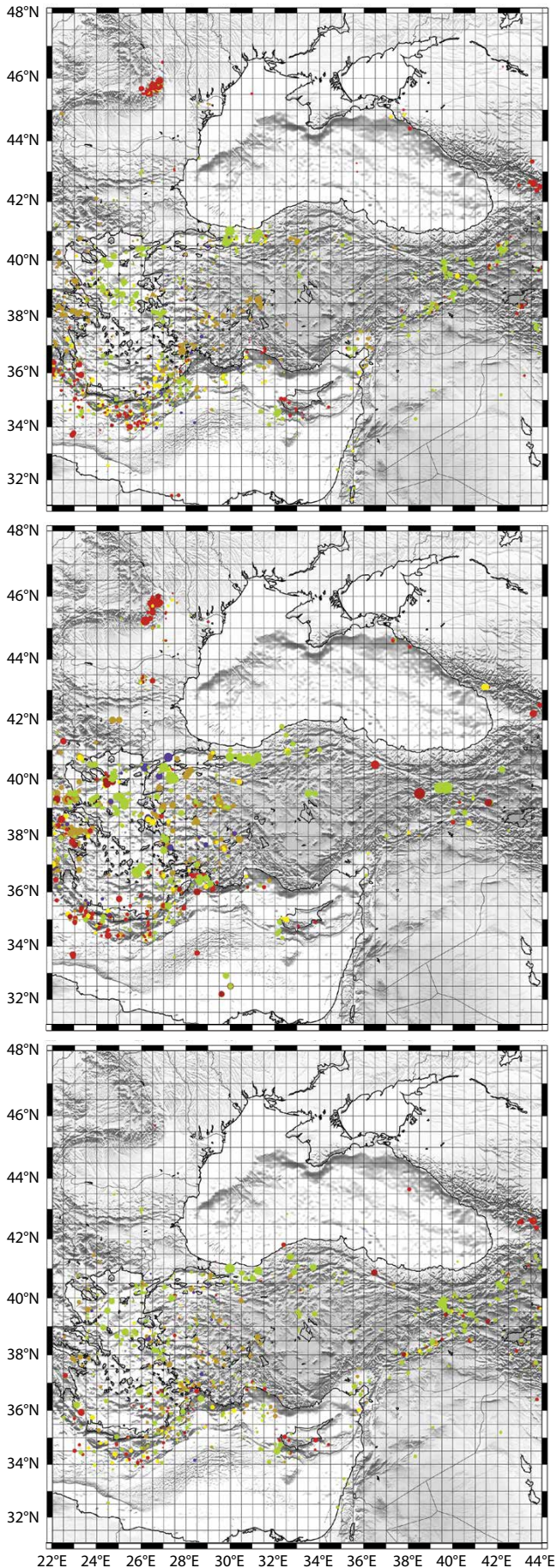
Figure 1. Fault types in the Eastern Mediterranean, Aegean, and Black Seas according to Zoback (1992) derived from (top) International Seismological Centre (ISC; http://www.isc.ac.uk), (middle) Earthquake Mechanisms of the Mediterranean Area (EMMA; Vannucci and Gasperini, 2004), and (bottom) Kalafat et al. (2009) moment tensor catalogs. NF = Normal faulting. NS = Normal faulting combined with considerable strike-slip component. TF = Thrust faulting. TS = Thrust faulting combined with considerable strike-slip component. SS = Strike-slip faulting. U = Unclassified type of faulting. See Table 1 for further information.

NF	· M = 4
NS	∘ M = 5
TF	∘ M = 6
TS	◯ M = 7
SS	◯ M = 8
U	

Yolsal and Taymaz (2010) showed that the period and shape of the first wave stayed very much the same for all dip angles. Titov et al. (1999) also reported that variations in the rake angle do not affect the tsunami waves significantly. In particular, they considered five different rake angles ranging from pure dip-slip mechanism (rake = 90°) to a 50% strike-slip component in the fault motion (rake = 135°), and concluded that the smallest amplitude (rake = 135°) is only 20% less than the largest (for rake = 90°).

Okal and Synolakis (2004) provided the first comprehensive attempt at understanding the effect of source parameter variation on tsunami generation. They let each parameter in their simulation—size of the earthquake (moment tensor, or M_o), hypocentral depth (h), fault slip (λ), fault dip (δ), fault strike (Φ), distance (L), ocean depth (H), and beach slope (β)— vary separately in order to isolate and study its individual influence on the amplitude and distribution of runup along the coast. The aim was to identify potential discriminants between landslide and dislocation (earthquake) sources based on two dimensionless quantities I_1 and I_2, where I_1 scales the maximum runup on the beach to the amplitude of seismic slip on the fault, and I_2 characterizes the aspect ratio of the distribution of runup on the beach. They found that a reduction in dip angle could result in a modest increase in the discriminants, primarily because a lower fault dip (δ) value results in a shallower average depth of the rupture area, and thus a larger static displacement above the source. In their investigation of fault slip (λ) variation, they observed that the strike-slip component lowers the value of I_1 as it reduces vertical static displacement. Finally, fault strike (Φ) was found to have only a

minimal impact on the discriminants.

Dao and Tkalich (2007) investigated the effects of astronomic tide, sea-bottom friction, Coriolis force, spherical coordinates, and wave dispersion. They showed that astronomic tide and bottom friction may have large impacts on tsunami propagation in shallow waters, whereas dispersion can lead to a notable change in amplitude of a tsunami propagating a large distance in deep water. They also showed that Coriolis force and spherical coordinate effects are smaller compared to other processes affecting tsunamis.

Okal and Synokalis (2008) evaluated far-field tsunami hazard in the Indian Ocean basin based on hydrodynamic simulations of 10 case studies of possible mega-earthquakes at major seismic zones surrounding the basin. In a series of numerical experiments in which the source parameters of the 2004 Sumatra tsunami were allowed to vary one by one, while keeping the seismic moment and the fault orientation unchanged, they determined that the main patterns of far-field tsunami amplitudes are remarkably robust with respect to nominal variations in parameters such as hypocentral depth, exact centroid location, and slip distribution on the fault plane.

Yolsal and Taymaz (2010) used numerical sensitivity tests to check the effects of earthquake source parameters on tsunami generation and wave characteristics resembling the historic 1303 Crete (M ~ 8.0) earthquakes. They considered three scenarios with different sets of fault plane parameters ($\Phi/\delta/\lambda$ as 115°/45°/110°, 220°/40°/140°, and 150°/40°/95°, respectively). By changing earthquake focal depths in their simulations to 5 km, 10 km, and 20 km while keeping other parameters the same, they showed that focal depth has a major effect on tsunami wave

Table 1. Classification of the focal mechanisms based on *P* (maximum compressive stress), *T* (minimum compressive stress), and *B* (intermediate stress or null) axes plunges according to Zoback (1992) as shown in Kiratzi et al. (2007).

Plunge of Axes		Faulting Type
P Axis	*T* Axis	
pl ≥ 52°	pl ≤ 35°	Normal Faulting [NF]
40° ≤ pl ≤ 52°	pl ≤ 20°	Normal faulting combined with considerable strike-slip component [NS]
pl ≤ 35°	pl ≥ 52°	Thrust faulting [TF]
pl ≤ 20°	40° ≤ pl ≤ 52°	Thrust faulting combined with considerable strike-slip component [TS]
pl ≤ 40° (and plunge of *B* axis pl ≥ 45°)	pl ≤ 40°	Strike-slip faulting [SS]
All *P*, *T*, and *B* axes plunge in the range 25° < pl < 45° or both *P* and *T* axes plunge in the range 40° < pl < 50°		Unclassified type of faulting [U]

characteristics in the far field. To test the significance of earthquake location, they selected two possible source locations for the Crete earthquake and calculated synthetic tsunami waves at selected affected areas. They found that tsunami characteristics such as wave height, shape, and travel time varied even when earthquake source parameters such as focal mechanism, source depth, and vertical displacement remained fixed. Their analysis suggests that final tsunami wave amplitudes can be affected by variations in bathymetry along the propagation direction, despite identical initial wave amplitudes. Thus, variation in earthquake location affects tsunami wave amplitude, wave energy distribution, and arrival times of initial waves calculated at the same pseudo-tide gauge points. In their investigation of the variation of the focal mechanism parameters, their observation was limited to the orthogonal tsunami propagation with respect to fault plane direction. Concerning variation in vertical displacement, their simulation showed increasing tsunami wave amplitudes with increasing vertical

displacements, as expected from theory. Yolsal and Taymaz (2010) also found that tsunami wave amplitudes changed considerably with varying focal depths at 5 km, 10 km, and 20 km. They concluded that the most critical parameter affecting tsunami wave characteristics is seismic moment (M_o) because tsunami wave amplitude and shape develop in direct proportion to the variation of magnitude and seismic moment of tsunamigenic earthquakes. They also discussed the effect of the bathymetry on tsunami wave propagation in both near and far fields, but because their study did not include high-resolution bathymetry, this conclusion is not justified. Considering the influence of focal mechanism solutions on amplitude, frequency content, and arrival times of tsunami waves in the far field, Yolsal and Taymaz (2010) pointed out that the dip and rake angles are key parameters that control the crest/depression for the (leading) tsunami waves. Variations in maximum displacement, focal depth, and faulting area changed tsunami wave amplitudes, though the theoretical arrival times remained almost the same.

SENSITIVITY STUDY SETTING

For this study, we selected a large lower-crust earthquake that occurred on August 8, 1303, in the Eastern Mediterranean as the reference event (case 1). It caused widespread damage and is one of the largest and best-documented seismic events in the history of the Mediterranean area (Yolsal et al., 2007). It has been suggested that the epicenter was probably near the island of Crete, and after this event, tsunami waves were reported not only at Crete but also as far away as the he Alexandria–Nile delta (Egypt), Peleponnese, Rhodes, Antalya (Southwest Turkey), and Acre, though not at Cyprus (Ambraseys, 2009). On the island of Crete, the sea rushed toward Candia (Heracleon) with such a force that many buildings collapsed and many people were killed. In Alexandria, Egypt, the worst damage was caused by a combination of the earthquake, the sea, and high winds, which drove ships onto the coast and demolished part of the rampart, killing 46 people. Ships sailing in the middle of the Nile and lying at anchor were thrown onto the banks (Soloviev et al., 2000; Altınok et al., 2011). The tsunami was observed on the island of Rhodes and in the Adriatic Sea (Soloviev et al., 2000). In Acre (today's Israel), the sea receded more then 1.6 km from the coast, and it also retreated in the harbors of today's Syria and Lebanon. Papadopoulos (2011) provides a detailed discussion of this earthquake and associated tsunami. Earthquake and associated damage distributions are also listed in most descriptive and parametric catalogs for the Mediterranean basin (Taymaz et al., 1990, 1991; Ozel et al., 2011).

Geologically, the orientations of active faults vary along the concave part of the Hellenic arc (e.g., Pliny and Strabo Trenches) in accordance with subduction of remnants of an old lithospheric slab (Taymaz et al., 1990, 1991). Hence, the Hellenic Trench in the vicinity of Crete is considered to be a seismogenic zone of considerable importance in the Mediterranean region. In this study, we consider 14 different cases (Figure 2) composed of various strike (Φ; 45°, 60°, 75°), dip (δ; 15°, 45°, 30°, 60°), and rake (λ; 30°, 50°, 70°, 90°, 110°, 130°, 150°) values to investigate the effects of the fault orientation-focal mechanism variation in tsunami generation and propagation in the Eastern Mediterranean. Table 2 provides all source parameters defined for the reference event based on our interpretation of the 1303 Crete event (case 1).
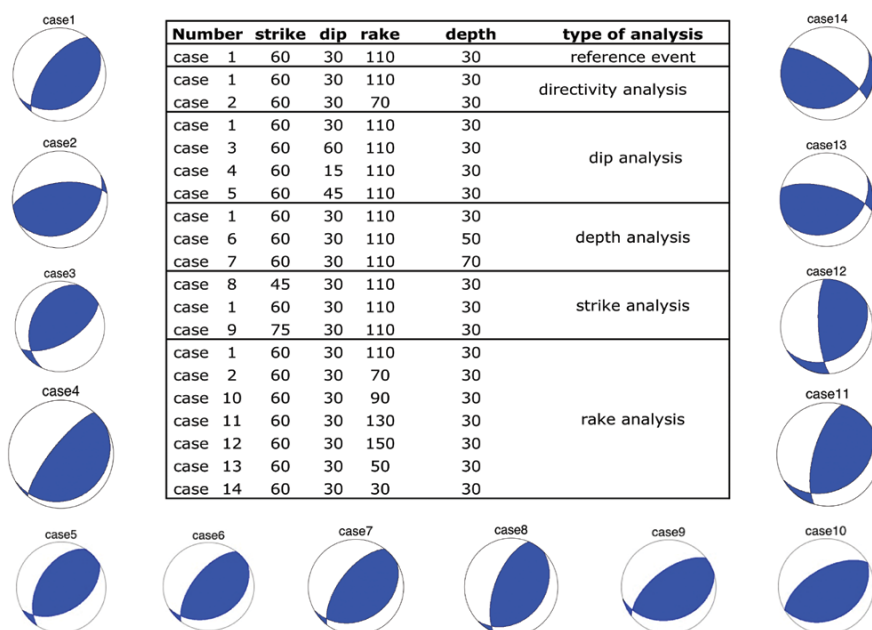

Number		strike	dip	rake	depth	type of analysis
case	1	60	30	110	30	reference event
case	1	60	30	110	30	directivity analysis
case	2	60	30	70	30	
case	1	60	30	110	30	
case	3	60	60	110	30	dip analysis
case	4	60	15	110	30	
case	5	60	45	110	30	
case	1	60	30	110	30	
case	6	60	30	110	50	depth analysis
case	7	60	30	110	70	
case	8	45	30	110	30	
case	1	60	30	110	30	strike analysis
case	9	75	30	110	30	
case	1	60	30	110	30	
case	2	60	30	70	30	
case	10	60	30	90	30	
case	11	60	30	130	30	rake analysis
case	12	60	30	150	30	
case	13	60	30	50	30	
case	14	60	30	30	30	

Figure 2. Focal mechanism parameters for 14 selected cases composed of various combinations of strike (Φ; 45°, 60°, 75°), dip (δ; 15°, 45°, 30°, 60°) rake (λ; 30°, 50°, 70°, 90°, 110°, 130°, 150°), and depth (30 km, 50 km, 70 km) values and corresponding beach-ball displays. Case 1 is the reference for comparing 13 other cases regarding tsunami generation with respect to source parameter variation. See Table 2 for all source parameters defined for case 1. Cases 6 and 7 refer to different depths with respect to case 1. In cases 2–5 and 8–14, one of the $\Phi/\delta/\lambda$ values has been modified, and the depth has been kept the same.

Table 2. Source parameters using case 1 as the reference in comparing 13 other cases to determine tsunami generation with respect to source parameter variation.

Lat	Lon	M_W	Depth	Displacement	Strike	Dip	Rake
34.7925°N	26.2093°E	8.0	30 km	9 m	60°	30°	110°

L = 100 km; W = 30 km; Fault area = 3,000 km^2; Rock Rigidity = 5E+11 dyn cm^{-2}.
Seismic Moment = 1.35E+21 Newton-Meter = 1.35E+28 dyne-centimeter

TSUNAMI MODELING

Our study uses the NAMI DANCE Tsunami Simulation and Visualization Code with nonlinear shallow water equations with spherical coordinates to investigate the sensitivity of earthquake source parameters in tsunami generation and propagation. This code is based on

the solution of a nonlinear form of the long wave equations with respect to related initial and boundary conditions. Nobuo Shuto and Fumihiko Imamura developed the important TUNAMI N2 model, which is now available to tsunami scientists under the UNESCO umbrella (Imamura, 1989; Shuto et al., 1990; Goto and Ogawa, 1991). TUNAMI N2 determines tsunami source characteristics from earthquake rupture characteristics. It computes all necessary parameters of tsunami behavior in shallow water and in the inundation zone, permitting a better understanding of bathymetry's effect on tsunamis. Andrey Zaytsev, Anton Chernov, Ahmet Yalciner, Efim Pelinovsky, and Andrey Kurkin developed NAMI DANCE using the identical computational procedures of TUNAMI N2. We obtained 30 arc-sec (approximately 900 m) resolution bathymetry data from GEBCO and gridded it using the Surfer application. Source files are created in NAMI DANCE and exact locations of virtual gauge points (GPs) are determined using Surfer (Figure 3 shows the GPs used in this study). Calculations are performed at the nearest possible locations to the selected tsunami focal points (TFPs) within a ≈ 50–100 m bathymetry level. The time step parameter in NAMI DANCE is defined as the time interval for the simulation initiated by the source overlaid to the input bathymetry, for which a value of 2 has been assigned in the analysis. The duration of the simulation is set at 120 minutes to try to cover a considerable part of tsunami lifetime, and output GRD files (Surfer grid format) are produced every 60 seconds. Further info about NAMI DANCE is available at http://namidance.ce.metu.edu.tr.

Figure 4 displays the initial tsunami

sources, maximum wave height distributions, and initial tsunami arrival times for all the cases considered in this study, showing the effects of focal parameter variation. Figure 5 presents time histories of water level at selected GPs (red dots in Figure 3), showing the effects of changes in strike, dip, rake, and depth parameters.

Effect of Strike (Φ) Variation in Tsunami Generation

We used cases 1, 8, and 9 to analyze the effect of strike variation on tsunami generation by changing the strike (Φ) to 45°, 60°, and 75° while keeping other parameters (dip, rake, depth) constant (Figure 2). Our simulations indicate that strike variation affects tsunami arrival time by about five minutes when only GPs are considered. Note that the range of changes applied in the strike analysis is narrower in comparison to other parameters investigated in this study, and it mainly corresponds to a minor deviation from the fault plane orthogonal, which is perpendicular to the main bathymetric structure in the region—the

eastern section of the Hellenic Arc between Crete and Rhodes. Wider strike parameter ranges could lead to different conclusions, but the strike of a tsunamigenic fault in a tectonic setting is likely the best known parameter of those selected in this study. In this narrow band of variation, Figure 5 shows that a change in strike strongly affects the tsunami amplitude in the impact zone, suggesting that it is important to consider an earthquake fault's strike in any tsunami hazard assessment.

Effect of Dip (δ) Variation in Tsunami Generation

We used cases 1, 3, 4, and 5 to analyze the effect of dip variation on tsunami generation by changing the dip (δ) to 15°, 30°, 45°, and 60° and keeping other parameters (strike, rake, depth) constant (Figure 2). The maximum wave amplitude was lower for the smaller dip value (≈ 50% in the near field), and no effect on arrival time was observed, a result in accordance with Titov et al. (1999). On the other hand, these results contradict the argument of Okal and Synolakis
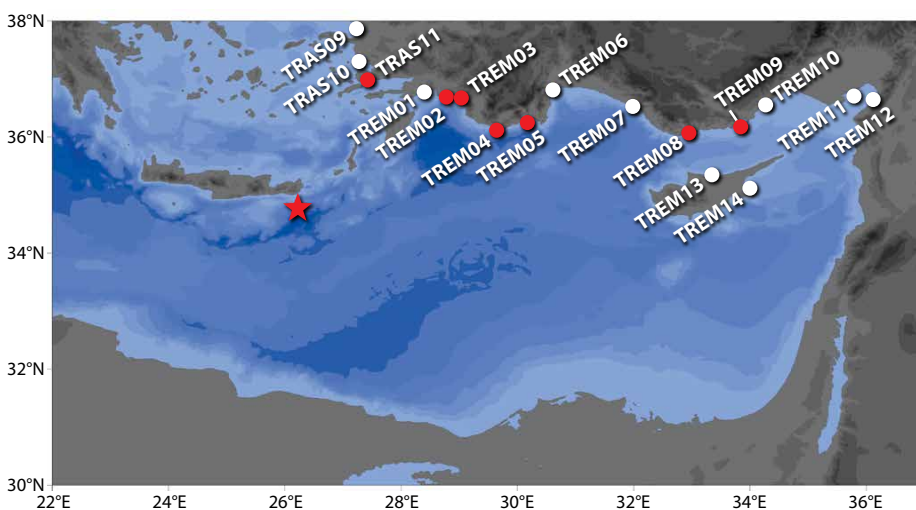

Figure 3. Gauge points in the Eastern Mediterranean used in this study. Mareograms of selected gauge points (red circles) are used for comparison purposes (Figure 5). The red star indicates the epicenter of the 1303 Crete earthquake selected for this study. Table 2 provides the corresponding earthquake source parameters. See Table 3 for additional details on these gauge points.

(2004) that a lower value of δ would result in a shallower average rupture area depth, and thus a larger static displacement above the source.

Effect of Rake (λ) Variation in Tsunami Generation

We used cases 1, 2, 10, 11, 12, 13, and 14 to analyze the effect of rake variation on tsunami *generation* by changing the rake (λ) to 30°, 50°, 70°, 90°, 110°, 130°, and 150°, representing thrust/thrust oblique faulting and keeping other parameters (strike, dip, depth) constant (Figure 2). Simulated mareogram recordings indicate that the arrival time of the initial wave remains constant and is not affected by rake variation. On the other hand, a change of 120° causes a 50% increase in maximum wave amplitude in the near field and a 10-minute delay in arrival time. This phenomenon is also observed in the far field if significant wave arrival occurs. Rake variations representing normal/normal oblique faulting (λ= –30°, –50°, –70°, –90°, –110°, –130°, –150°) would lead to a mirror image of what has been simulated for thrust/thrust oblique faulting. This could also lead to the conclusion that for a given magnitude, expected maximum and minimum tsunami wave amplitudes could be evaluated from a waveform envelope rather than limited to a single point in time or amplitude to derive the worst-case scenario. It may be especially important to accommodate rake uncertainties in tsunami hazard studies, especially in regions such as the Eastern Mediterranean, where devastating historical tsunamis took place but no modern-day tsunami disaster has been witnessed.

Effect of Depth (H) Variation in Tsunami Generation

Finally, we used cases 1, 6, and 7 to analyze the effect of depth variation on tsunami generation by changing the depths to 30 km, 50 km, and 70 km and keeping other parameters (strike, dip, rake) constant (Figure 2). Resulting simulations indicate maximum wave amplitude approximately 50% lower for 70 km depth compared to 30 km depth. These results are considerably different from those of Okal (1988), who showed

Table 3. Descriptive information on gauge points (GPs) in the Eastern Mediterranean used in this study together with the summary results of the simulations, including arrival times and amplitudes of initial and maximum waves. (M) indicates that an actual tide gauge station is located at the site. Simulated mareograms for a subset of GPs based on different focal mechanisms are shown in Figure 5 for comparison purposes.

Gauge Point Code	Gauge Point Name	Gauge Point Depth (m)	Lon (E)	Lat (N)	Arrival time of initial wave (min)	Arrival time of max. wave (min)	Maximum (+) amp. (m)	Maximum (−) amp. (m)
TRAS09	Kusadasi	61.2	27.2280°	37.8608°	91	91	0.01	−0.02
TRAS10	Didim	53.1	27.2736°	37.2964°	70	85	0.09	−0.03
TRAS11	Bodrum (M)	56.2	27.4227°	36.9739°	36	89	0.45	−0.61
TREM01	Aksaz (M)	68.9	28.4013°	36.7645°	21	43	0.33	−0.31
TREM02	Dalaman	103.9	28.7784°	36.6793°	15	37	0.32	−0.20
TREM03	Fethiye	68.0	29.0405°	36.6597°	19	41	0.37	−0.44
TREM04	Kas	52.4	29.6421°	36.1052°	13	37	0.21	−0.16
TREM05	Finike	50.2	30.1661°	36.2418°	20	43	0.21	−0.17
TREM06	Antalya (M)	57.8	30.6052°	36.8088°	39	112	0.29	−0.21
TREM07	Alanya	55.2	31.9859°	36.5248°	40	62	0.21	−0.13
TREM08	Mersin Bozyazi (M)	62.7	32.9437°	36.0690°	51	75	0.23	−0.19
TREM09	Mersin Tasucu (M)	53.6	33.8431°	36.1692°	76	97	0.15	−0.14
TREM10	Mersin Erdemli (M)	55.1	34.2712°	36.5491°	93	115	0.18	−0.01
TREM11	Yumurtalık	49.6	35.7855°	36.6989°	0	0	0.00	0.00
TREM12	Iskenderun	53.1	36.1281°	36.6325°	0	0	0.00	0.00
TREM13	Girne	58.7	33.3407°	35.3431°	54	78	0.19	−0.15
TREM14	Gazimagusa	54.0	33.9941°	35.1188°	80	99	0.07	−0.09

tsunami wave amplitude reduced by a factor of two when focal depth was increased by a factor of five, from 20 km to 100 km. This ambiguity shows that focal depth variation's effect on tsunami generation could be related to ocean depth and bathymetry. Similar assessments need to be made in each basin prone to tsunami hazard. Our results also suggest that special emphasis should be given to identifying depth phases in regional distances to better determine actual hypocenter depth. Last but not

least, tsunami scenario databases used in hazard assessment or tsunami early warning systems should be developed considering various earthquake source ranges in accordance with the tectonic setting of these sources.

CONCLUSIONS

Previous studies conducted in different parts of the globe indicate that the main characteristics of tsunami propagation are unique for each basin. In this study, we attempted a comprehensive analysis

of the effect of variations in earthquake focal mechanism parameters on tsunami generation, with special focus on the Eastern Mediterranean. Our analysis shows that given the uncertainties in focal mechanism parameters, tsunami hazard studies should be based on a range of these parameters where the maximum generated tsunami would be taken into consideration. If computational limitations are considered, at least sensitivity studies, such as those presented here, should be conducted,
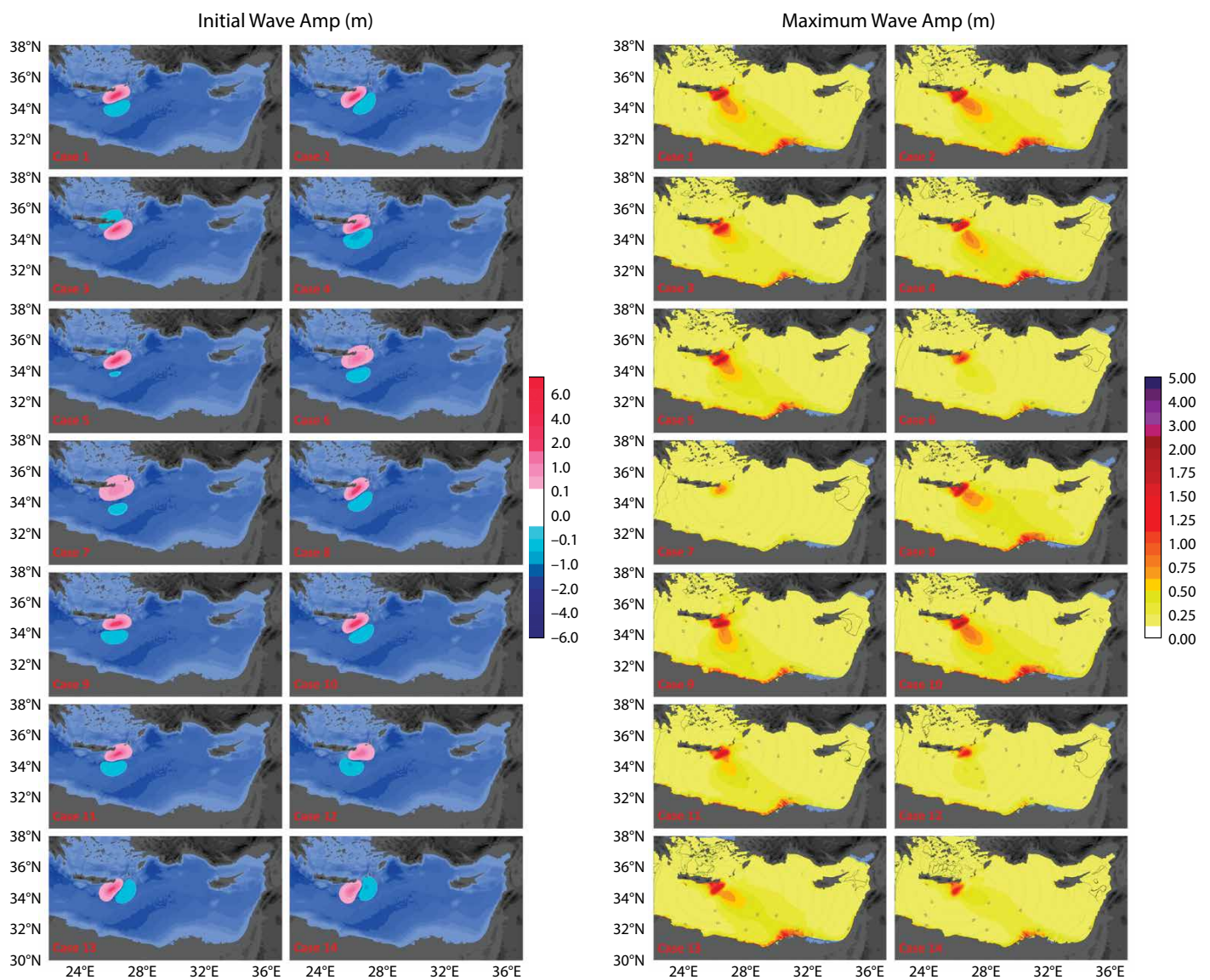

Figure 4. (left panels) Initial tsunami sources and (right panels) maximum wave height distributions and initial tsunami arrival times for all the cases considered in this study, showing the effects of the focal parameter variation. Fault strike controls the direction and focusing of tsunami propagation due to its orthogonality property.

and parameters should be selected that would lead to maximum tsunami generation. Another option would be to consider only strike and rake variations in the scenario databases as the key criteria in determining the worst-case scenario for a given forecast point. It should also be noted that the synthetic measurements obtained at the gauge points in the absence of high-resolution bathymetric data should be considered only as overall guidance. Our results demonstrate the importance of the accuracy of earthquake source parameters in making reliable tsunami predictions and the need for high-resolution bathymetric data to enhance accuracy. This study did not address other earthquake
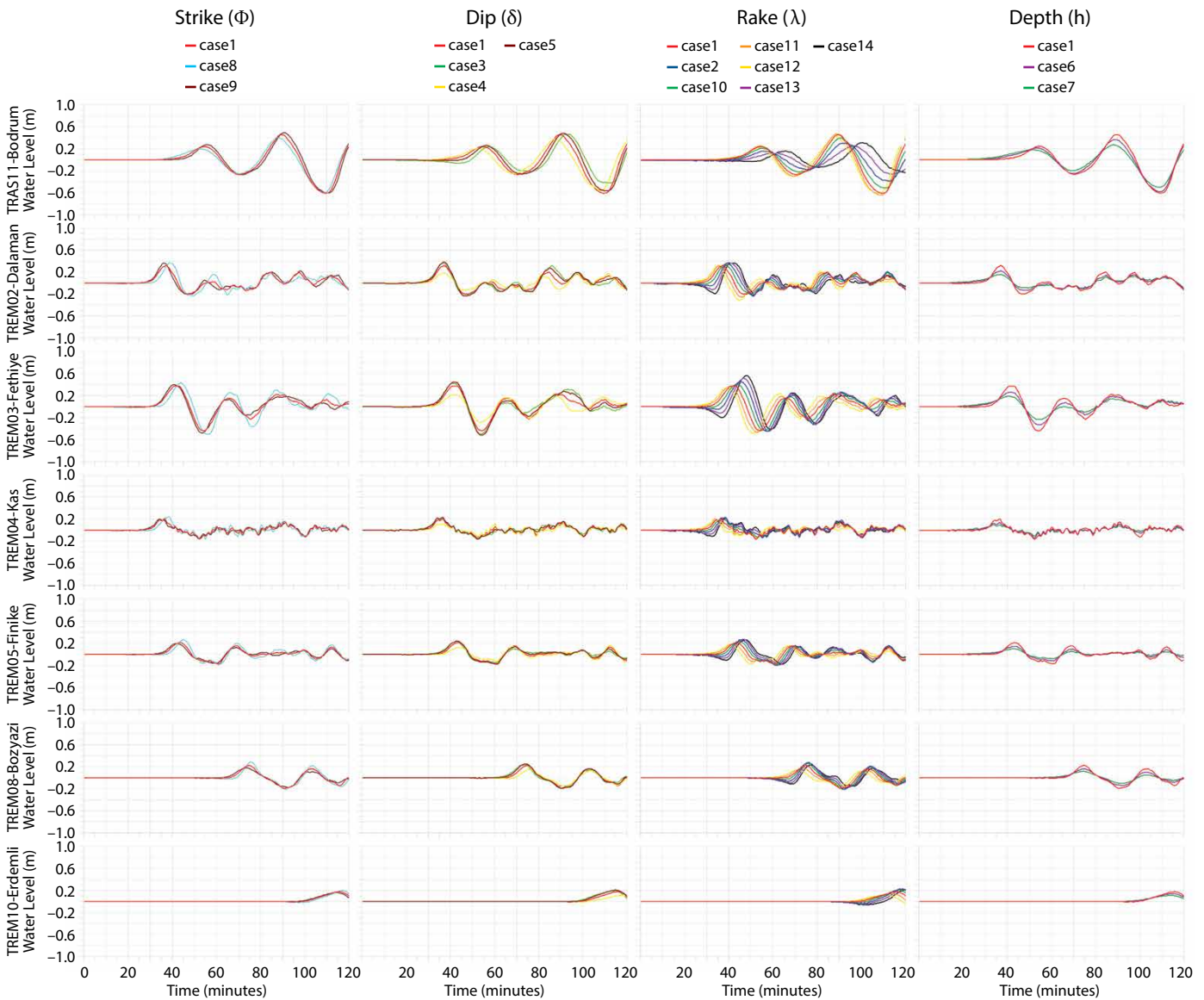
Figure 5. Time histories of water level at selected gauge points (red dots in Figure 3), showing the effect of changes in strike, dip, rake, and depth. Simulated mareograms are sorted from top to bottom by distance from source to gauge points. Each column indicates the parameter changed, and in each column, each row indicates a gauge point (GP), which is the coastal point where the effect of the change in the parameter is simulated. There are seven GPs and, from top to bottom in each column, they are sorted by distance from the earthquake. Each scenario (case) has a unique combination of strike, dip, rake, and depth parameter. Cases 1, 8, and 9 were used in the strike analysis, corresponding to changes in strike values of 60°, 45°, and 75°, respectively. All other parameters (dip, rake, depth) remained constant. Cases 1, 3, 4, and 5 were considered in the dip analysis, corresponding to changes in dip values of 30°, 60°, 15°, and 45°, respectively. All other parameters (strike, rake, depth) remained constant. Cases 1, 2, 10, 11, 12, 13, and 14 were considered in the rake analysis, corresponding to changes in rake values of 110°, 70°, 90°, 130°, 150°, 50°, and 30°, respectively. All other parameters (strike, dip, depth) remained constant. Cases 1, 6, and 7 were considered in the depth analysis, corresponding to changes in depth values of 30 km, 50 km, and 70 km, respectively. All other parameters (strike, dip, rake) remained constant.

parameters, such as heterogeneous slip distribution and rupture duration, which affect tsunami initiation and propagation. Uncertainties in these parameters are far greater than for those considered in this study; thus, their use in deterministic tsunami hazard studies may not be suitable, despite their benefits for promoting understanding of the coupling of seismic displacement with tsunami generation.

REFERENCES
Abe, K., and M. Okada. 1995. Source model of the Noto-Hanto-Oki earthquake tsunami of 7 February 1993. *Pure and Applied Geophysics* 144:621–631, http://dx.doi.org/10.1007/BF00874386.

Altınok, Y., B. Alpar, N. Ozer, and H. Aykurt. 2011. Revision of the tsunami catalogue affecting Turkish coasts and surrounding regions. *Natural Hazards and Earth Systems Sciences* 11:273–293, http://dx.doi.org/10.5194/nhess-11-273-2011.

Ambraseys, N.N. 2009. *Earthquakes in the Mediterranean and Middle East*. Cambridge University Press, 968 pp.

Dao, M.H., and P. Tkalich. 2007. Tsunami propagation modeling—A sensitivity study. *Natural Hazards and Earth Systems Sciences* 7:741–754, http://dx.doi.org/10.5194/nhess-7-741-2007.

Frohlich, C., and S.D. Davis. 1999. How well constrained are well-constrained T, B, and P axes in moment tensor catalogs? *Journal of Geophysical Research* 104(B3):4,901–4,910, http://dx.doi.org/10.1029/1998JB900071.

Gica, E., M.H. Teng, M. Asce, P.L.-F. Liu, F. Asce, V.V. Titov, and H. Zhou. 2007. Sensitivity analysis of source parameters for earthquake generated distant tsunamis. *Journal of Waterways, Port, Coasts and Ocean Engineering* 133:429–441, http://dx.doi.org/10.1061/(ASCE)0733-950X(2007)133:6(429).

Goto, C., and Y. Ogawa. 1991. *Numerical Method of Tsunami Simulation With the Leap-Frog Scheme* (translated for the TIME Project by N. Shuto). Disaster Control Research Center, Faculty of Engineering, Tohoku University, Sendai, Japan.

Helffrich, G.R. 1997. How good are routinely determined focal mechanisms? Empirical statistics based on a comparison of Harvard, USGS and ERI moment tensors. *Geophysical Journal International* 131:741–750, http://dx.doi.org/10.1111/j.1365-246X.1997.tb06609.x.

Imamura, F. 1989. *Tsunami Numerical Simulation with the Staggered Leap-frog Scheme (Numerical code of TUNAMI-N1)*. School of Civil Engineering, Asian Institute Technical and Disaster Control Research Center, Tohoku University.

Kalafat, K., K. Kekovali, Y. Gunes, M. Yilmazer, M. Kara, P. Deniz, M. Berberoglu. 2009. *A Catalogue of Source Parameters of Moderate and Strong Earthquakes for Turkey and its Surrounding Area (1938–2008)*. Bogazici University Press.

Kiratzi A., C. Benetatos, and Z. Roumelioti. 2007. Distributed earthquake focal mechanisms in the Aegean Sea. *Bulletin of the Geological Society of Greece* 40:1,125–1,137.

Okal, E.A. 1988. Seismic parameters controlling farfield tsunami amplitudes: A review. *Natural Hazards* 1:67–96, http://dx.doi.org/10.1007/BF00168222.

Okal, E.A., and C.E. Synolakis. 2004. Source discriminants for near-field tsunamis. *Geophysical Journal International* 158:899–912, http://dx.doi.org/10.1111/j.1365-246X.2004.02347.x.

Okal, E.A., and C.E. Synolakis. 2008. Far-field tsunami hazard from mega-thrust earthquakes in the Indian Ocean. *Geophysical Journal International* 172:995–1,015, http://dx.doi.org/10.1111/j.1365-246X.2007.03674.x.

Ozel, N.M., O. Necmioglu, A.C. Yalciner, D. Kalafat, and M. Erdik. 2011. Tsunami hazard in the Eastern Mediterranean and its connected seas: Toward a tsunami warning center in Turkey. *Soil Dynamics and Earthquake Engineering* 31:598–610, http://dx.doi.org/10.1016/j.soildyn.2010.11.005.

Papadopoulos, G. 2011. *A Seismic History of Crete*. Ocelatos Editions, 416 pp.

Satake, K. 1985. Effects of station coverage on moment tensor inversion. *Bulletin of the Seismological Society of America* 75:1,657–1,667.

Shuto, N., C. Goto, and F. Imamura. 1990. Numerical simulation as a means of warning for near-field tsunamis. *Coastal Engineering in Japan* 33(2):173–193.

Soloviev, S.L., O.N. Solovieva, C.N. Go, K.S. Kim, and N.A. Shchetnikov. 2000. *Tsunamis in the Mediterranean Sea 2000 BC–2000 AD*. Advances in Natural and Technological Hazards Research, vol. 13, Springer, 237 pp.

Taymaz, T., J.A. Jackson, and D. McKenzie. 1991. Active tectonics of the north and central Aegean Sea. *Geophysical Journal International* 106:433–490, http://dx.doi.org/10.1111/j.1365-246X.1991.tb03906.x.

Taymaz, T., J.A. Jackson, and R. Westaway. 1990. Earthquake mechanisms in the Hellenic Trench near Crete. *Geophysical Journal International* 102:695–731, http://dx.doi.org/10.1111/j.1365-246X.1990.tb04590.x.

Titov, V.V., H.O. Mofjeld, F.I. Gonzalez, and J.C. Newman. 1999. *Offshore Forecasting of Hawaiian Tsunamis Generated in Alaskan-Aleutian Subduction Zone*. NOAA Technical Memorandum ERL PMEL-114, Pacific Marine Environmental Laboratory, USA, 26 pp., http://www.pmel.noaa.gov/pubs/PDF/tito2049/tito2049.pdf.

Vannucci, G., and P. Gasperini. 2004. The new release of the database of Earthquake Mechanisms of the Mediterranean Area (EMMA Version 2). *Annals of Geophysics* Supplement to 47(1):307–334, http://gaspy.df.unibo.it/paolo/ATLAS/pages/EMMA_description.htm.

Yolsal, S., and T. Taymaz. 2010. Sensitivity analysis on relations between earthquake source rupture parameters and far-field tsunami waves: Case studies in the Eastern Mediterranean region. *Turkish Journal of Earth Sciences* 19:313–349.

Yolsal, S., T. Taymaz, and A.C. Yalcıner. 2007. Understanding tsunamis, potential source regions and tsunami-prone mechanisms in the Eastern Mediterranean. *Geological Society, London, Special Publications* 291:201–230, http://dx.doi.org/10.1144/SP291.10.

Zoback, M.L. 1992. First- and second-order patterns of stress in the lithosphere: The World Stress Map project. *Journal of Geophysical Research* 97(B8):11,703–11,728, http://dx.doi.org/10.1029/92JB00132.